European Journal of Soil Science, December 2008, **59,** 1063–1075 doi: 10.1111/j.1365-2389.2008.01061.x

The influence of bioturbation on the vertical distribution of soil organic matter in volcanic ash soils: a case study in northern Ecuador

F. H. Tonneijck[a] & A. G. Jongmans[b]
[a]*Institute for Biodiversity and Ecosystem Dynamics, University of Amsterdam, Nieuwe Achtergracht 166, 1018 WV Amsterdam, and*
[b]*Department of Environmental Science, Wageningen University, PO Box 47, 6700 AA Wageningen, the Netherlands*

Summary

Soil faunal bioturbation ('bioturbation') is often cited as a major process influencing the vertical distribution of soil organic matter (SOM). The influence of bioturbation on vertical SOM transport is complex because it is the result of interaction between different groups of soil faunal species that redistribute SOM through the soil profile in distinct ways. We performed a semi-quantitative micromorphological analysis of soil faunal pedofeatures and related their occurrence to the vertical distribution of SOM and high-resolution radiocarbon dating in volcanic ash soils under montane forest and grassland (páramo) vegetation in the northern Ecuadorian Andes. The páramo soil data suggest that bioturbation was largely responsible for the vertical distribution of SOM, while illuviation and root input were of minor importance. Bioturbation was caused by endogeic species, which typically mix the soil only over short vertical distances. Short vertical distance mixing was apparently enhanced by the upward shifting of bioturbation as a result of soil thickening due to SOM accumulation. A change from páramo to forest vegetation was accompanied by a change from endogeic to epigeic species. As these latter species do not redistribute material vertically, this eventually resulted in the formation of thick ectorganic horizons in the forest.

Introduction

The vertical distribution of SOM is principally determined by (i) the input – above and belowground – of litter, (ii) the output of organic matter through decomposition and (iii) its vertical transport. With respect to the latter, soil faunal bioturbation (further referred to as 'bioturbation') is often cited as a major process influencing the vertical distribution of SOM (e.g. Anderson, 1988; Lavelle, 1988; Rasse *et al*., 2006). Elzein & Balesdent (1995) demonstrated in a modelling study that bioturbation is the dominant mode of vertical transport, relative to leaching, in a range of soil types.

Soils formed in volcanic ash contain the largest amounts of SOM per unit area of all mineral soil orders (Dahlgren *et al*., 2004), making them potential carbon sinks for the greenhouse gas CO_2, which is of global importance. We previously investigated the age and vertical distribution of SOM in such soils under montane forest and grassland (páramo) vegetation in the northern Ecuadorian Andes (Tonneijck *et al*., 2006; Tonneijck *et al*., 2008). These soil profiles consist of a current soil in a thick tephra deposit superimposed on a SOM-rich palaeosol in a preceding tephra deposit. We observed a progressive downward increase in SOM from the relatively SOM-poor subsoil of the current soil into the SOM-rich top of the palaeosol, further referred to as the 'overprinted zone'. Vertical transport of dissolved OM by leaching can be assumed to be insignificant in volcanic ash soils, because of the large metal-to-SOM ratios that strongly limit its mobility (Aran *et al*., 2001; Dahlgren *et al*., 2004). Furthermore, rooting is typically superficial in Andean montane forests (Soethe *et al*., 2006) and páramo (Hofstede & Rossenaar, 1995). Therefore, the occurrence of the overprinted zone strongly suggested that bioturbation plays an important role during soil formation.

Correspondence: F. H. Tonneijck. E-mail: f.h.tonneijck@science.uva.nl
Received 13 February 2008; revised version accepted 18 June 2008

The influence of bioturbation on vertical SOM transport is complex because it is the result of interaction between different groups of soil faunal species. These may typically be divided into three main groups according to their behaviour in the soil (Anderson, 1988), similar to the classification for ecological groups of earthworms (Lee, 1959): epigeic, anecic and endogeic species. These groups of species redistribute SOM through the soil profile in distinct ways (Anderson, 1988; Lavelle, 1988; Lee & Foster, 1991). Epigeic species inhabit the ectorganic layers and do not actively redistribute material. Anecic species feed mainly on OM from the earth surface but inhabit deeper soil layers in which they create (semi-) permanent vertical burrows and therefore are responsible for transport of OM over large vertical distances that may exceed 1 m. By contrast, endogeic species ingest both mineral soil and organic matter and create extensive subhorizontal burrowing networks, thus transporting SOM only over short vertical distances. Some endogeic species are typically concentrated around 10–20 cm depth, other endogeic species occur deeper in the soil profile up to 50 cm depth.

To increase understanding of the influence of bioturbation on the vertical distribution of SOM in volcanic ash soils in northern Ecuador, we performed a semi-quantitative micromorphological analysis of soil faunal pedofeatures and related their occurrence to the vertical distribution of SOM and high-resolution radiocarbon dating.

Description of study area and sites

The study sites are located in the Guandera Biological Station in northern Ecuador, near the border with Colombia, on the west facing slopes of the eastern Cordillera (Figure 1 and Table 1, 0°35′ North and 77°41′ West). Guandera has a (semi-) natural upper forest line at approximately 3650 m above mean sea level. There are some forest patches above the current upper forest line. Dominant species within the forest are *Clusia flaviflora* ENGL., *Weinmannia cochensis* HIERON. and *Ilex colombiana* CUATREC. and the páramo is characterized by bunch-grass *Calamagrostis effusa* KUNTH (STEUD.) and stem-rosette *Espeletia pycnophylla* CUATREC. The forest and páramo belong to the globally leading Tropical Andes biodiversity 'hotspot' (Myers *et al*., 2000). Because deforestation in the Inter-Andean valleys has been particularly severe (Keese *et al*., 2007), the Guandera forest constitutes a unique remnant. Mean annual precipitation is around 1900 mm and mean annual temperature ranges from 12°C at 3000 m above sea level to 4°C at 4000 m above sea level. Both precipitation and temperature show little seasonal variation. The soil climate is isomesic and perudic.

We selected a site covered by forest (G1) at 3501 m above sea level, a site in a forest patch above the current upper forest line (G5a) at 3697 m above sea level, a site just next to it with páramo vegetation (G5b) and finally a site at 3860 m above sea level within the páramo (G7). We were able to identify soils with erosional/depositional features by anomalous grain size and geochemical data (Tonneijck *et al*., 2008) and only investigated undisturbed soils. The soil profiles at our sites were each formed in three distinct tephra deposits of Holocene age (Tonneijck *et al*., 2008). Related to this tephra stratigraphy all soils contained a multisequum consisting of a current soil, a palaeosol and a second heavily truncated or immature palaeosol, each at least 40 cm thick. Between the current soil and the first palaeosol an overprinted zone with transitional organic carbon contents, grain size distribution and element ratios was present. In the soil horizon designations we used '1/2' as a prefix to indicate this overprinted zone.

The mineral horizon sequence can be summarized as Ah1 – 1/2Ah2/1/2Bw – 2Ahb – 2Bwsb – 3BCb. In addition, the forest profiles had ectorganic horizons (LFH) with a combined thickness of up to 75 cm. By contrast, ectorganic horizons (L) barely

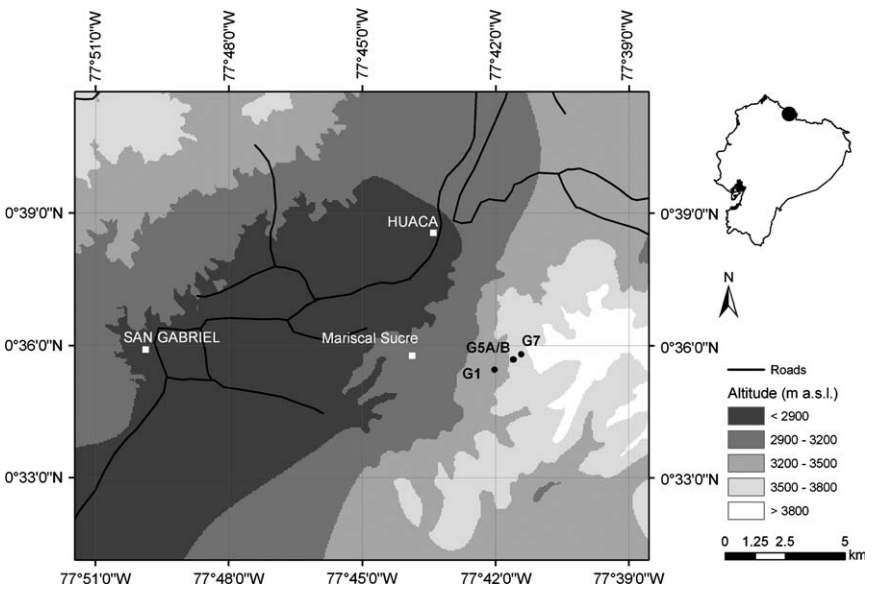

Figure 1 Map of study area and study sites. ● = study sites; ■ = village or town.

Table 1 Description of the study sites

Site	Altitude[a] (m above sea level)	Coordinates[b] (°)	Inclination (°)	Exposure (°)	Soil type WRB	Current vegetation
G1	3501 ± 9 (n = 20)	N 0°35′27″/W 77°42′1″	3	270	Histosol	Forest
G5a	3697 ± 9 (n = 9)	N 0°35′41″/W 77°41′36″	13	280	Cambisol	Forest patch in páramo
G5b	3694 ± 13 (n = 9)	N 0°35′41″/W 77°41′35″	8	280	Andosol	Páramo
G7	3860 (n = 1)	N 0°35′48″/W 77°41′25″	8	270	Andosol	Páramo

[a]Altitudes from altimeter.
[b]GPS coordinates in WGS 1984.

exceeded 1 cm in the páramo profiles. A thin placic horizon was present at the boundary between the first and second palaeosol. This placic horizon is ascribed to a strong textural contrast hindering drainage of the otherwise well drained soils. The soils were classified as a Histosol overlying a mineral soil with andic properties (G1), as an Andic Cambisol (G5a) and as an Andosol (G5b and G7) according to the World Reference Base (FAO, 2006). The ectorganic horizons were classified as resimor (G1) and mor (G5a) in the forest and as mull in the páramo (G5b and G7), according to Green *et al.* (1993). We observed that the ectorganic horizons changed abruptly from mor to mull at the boundary between forest (patch) and páramo.

Materials and methods

Sampling procedures

Soil pits of approximately 1.5 m^2 surface area and a depth of at maximum 2 m were dug. We took bulk soil samples for physical and chemical analyses (n = 35, for humic substances n = 28), ring samples for bulk density determination (n = 35) and undisturbed box samples (with dimensions of 7 cm height × 5 cm width × 4 cm depth) for the preparation of thin sections (n = 30, up to the top of the first palaeosol), in the same soil pit at regular depths but respecting horizon boundaries. Sampling depths are presented in Figure 2. Bulk and ring samples were taken over a vertical interval of 5 cm, the middle of which was noted as the depth of the sample. Additionally, we took undisturbed vertical soil samples (monoliths) using one or two metal gutters of 75 cm height × 5 × cm width × 4 cm depth. For radiocarbon dating (n = 35) and additional estimation of organic carbon contents (n = 182) and humic substances (n = 19, being a selection of the samples used for radiocarbon dating), samples were cored from the monoliths by means of corers of 0.5 cm and 0.75 cm diameter, respectively. As the continuous input of fresh OM into soils causes the measured ^{14}C ages of bulk SOM to be always somewhat younger than the depositional age (Wang *et al.*, 1996), it is

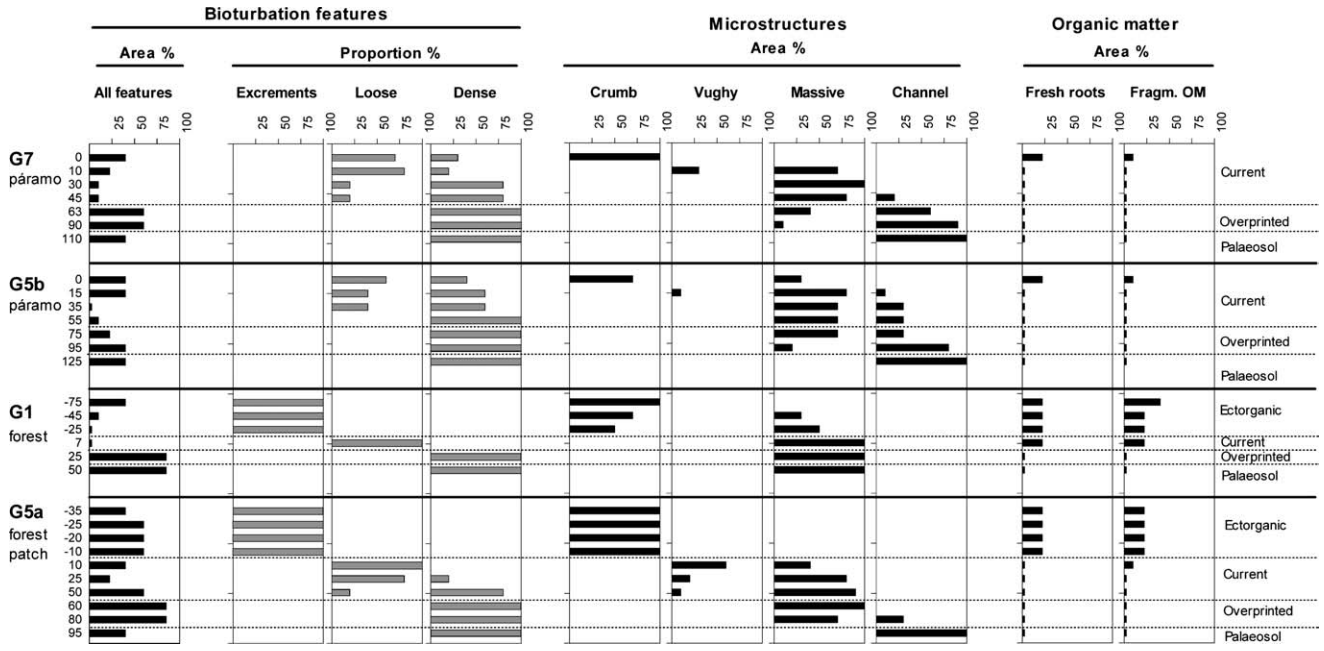

Figure 2 Bar graphs of bioturbation features (area %), type of bioturbation features (as proportions of total), microstructures (area %) and organic matter (area %) versus sample depth (cm, top of mineral soil set at zero) for all soil profiles.

necessary to use such small sampling intervals for radiocarbon dating. All samples were stored at 2°C under field moist conditions prior to analysis.

Laboratory procedures and statistical analysis

Laboratory procedures for the measurement of total carbon content, dry bulk density, pH ($CaCl_2$) and allophane content were described in Tonneijck *et al.* (2006) and Tonneijck *et al.* (2008). Total carbon equals organic carbon, because carbonates were absent. Humic substance fractions of SOM were obtained by alkali and subsequent acid extraction according to Schnitzer (1982). After each extraction, carbon content in the extract was measured with a Shimadzu TOC Analyser 5000 (Kyoto, Japan), to obtain the organic carbon content present in humic acids (HA). Pearson and Spearman correlations (bivariate) between total organic carbon and carbon in HA were calculated ($n = 47$) using the SPSS Correlate procedure and considered significant when $P < 0.01$. Field-moist undisturbed box samples were impregnated after replacing water by acetone, according to Miedema *et al.* (1974). Thin sections were prepared according to Murphy (1986).

Radiocarbon dating

In addition to the radiocarbon data already published (Tonneijck *et al.*, 2006; Tonneijck *et al.*, 2008), we performed dating for profiles G5a, G5b and G7 to further increase the vertical resolution and acquired a first set of ^{14}C dates for profile G1. Radiocarbon dating followed procedures outlined in Tonneijck *et al.* (2006). In short, humic substance fractions of SOM were radiocarbon dated with an Accelerator Mass Spectrometer. The fulvic acid fraction was discarded because of its inherent mobility in most soils. We previously discussed (Tonneijck *et al.*, 2006) that in Andosols lacking a thick ectorganic horizon, dating of HA gave the most accurate results because roots tend to accumulate in the residual (humin) fraction rather than in the HA fraction and HA was immobile due to the large metal/SOM ratios and acidic pH. Contrarily, in mineral soil samples just beneath thick ectorganic horizons, humin ages were more accurate, because HA was then contaminated by younger HA illuviated from the ectorganic horizons while roots were concentrated in the ectorganic horizons rather than in the mineral topsoil. Consequently, we dated HA in all cases, except for samples just beneath a thick ectorganic horizon where we dated both the HA and humin fractions. Radiocarbon ages were calibrated, according to procedures outlined in Tonneijck *et al.* (2006), to a calendar year probability distribution (cal AD/BC). Calibrated radiocarbon ages are expressed as the range of calendar years of the 1 sigma peak with the largest relative area under the probability distribution. As the ranges are small, calculations are performed with the mean and the dots displayed in the graphs represent the whole range of calendar years at the scale of the graph.

Micromorphological analysis

Thin sections were analysed using a Leitz M420 macrozoom microscope (for a magnification of 8x) and a Leitz Wetzlar petrographic microscope (for magnifications of 25x and 63x). Thin sections were described following the micromorphological terminology of Stoops (2003). Abundance classes were as follows: very few (< 5%), few (5–15%), common (15–30%), frequent (30–50%), dominant (50–70%) and very dominant (> 70%). To display these classes in bar graphs we used class midpoints. Rather than using Stoops' grades of coalescence of micro-aggregates, we preferred the more illustrative terminology of welding. Our single faunal excrements correspond to Stoops' very porous micro-aggregates and our very strongly welded excrements to very dense micro-aggregates. We grouped the terms 'organ residues', 'tissue residues' and 'cell residues' of Stoops in one class of 'fragmented OM', to increase readability. Fragmented OM includes both fresh and more decomposed (less birefringent) OM.

We defined soil faunal pedofeatures (i.e. excrements, loose infillings and dense infillings) as 'bioturbation features'. In addition, we included zones with a vughy microstructure (i.e. zones containing frequent vughs) in our definition, because these zones were interpreted to result from very strong welding of loose infillings, which is in accordance with observations by Pawluk (1987).

Results

Soil properties

General soil properties were reported in Tonneijck *et al.* (2008). Briefly, the upper mineral horizons were characterized by a very large organic carbon content (8–22%), acidic pH (pH $CaCl_2$ 3.2–4.4) and small dry bulk density (0.3–0.7 g cm^{-3}). The mineral topsoils did not contain allophane, while the subsurface horizons contained up to 5% allophane.

Vertical distribution of SOM and HA

The vertical distribution of total organic carbon and carbon in the HA fraction is presented in Figure 3a. As explained in the introduction, organic carbon content decreased with depth in the current soils, but instead of an abrupt increase in organic carbon content at the boundary with the palaeosol, organic carbon content increased gradually. Carbon in the HA fraction followed a similar distribution with depth as organic carbon and both Pearson and Spearman correlations between carbon in the HA fraction and total organic carbon were large (+0.82 and +0.86, respectively, $P < 0.001$ in both cases).

Radiocarbon dating

Conventional and calibrated radiocarbon ages are presented in Table 2, and Figure 3c additionally shows calibrated age versus depth for each soil profile. We used the calibrated radiocarbon

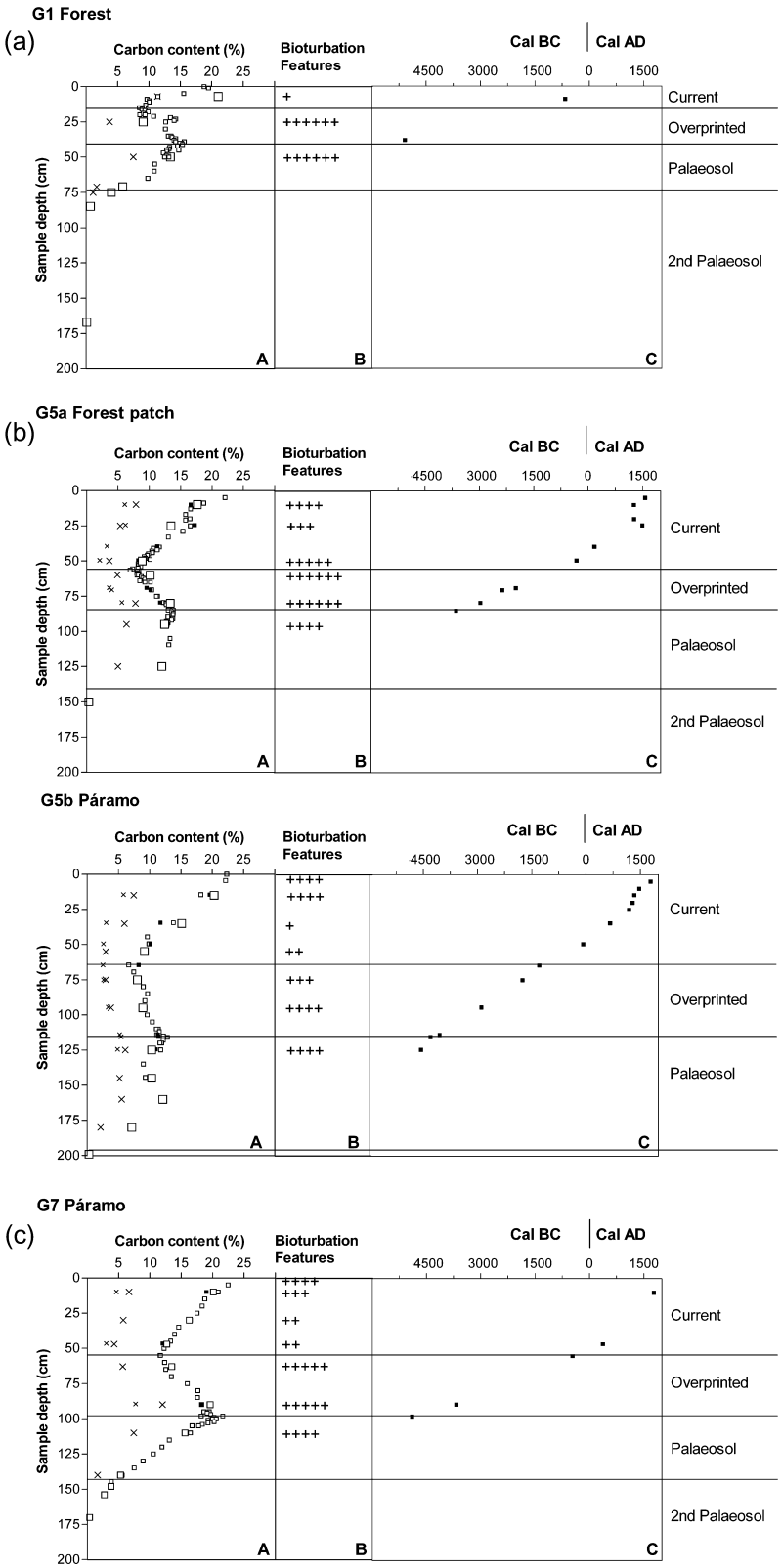

Figure 3 Vertical distribution of (a) total organic carbon content (%), □ = bulk sample (5 cm interval), □ = monolith sample (0.75 cm interval), ■ = ^{14}C sample (0.5 cm interval), and organic carbon content in humic acids (%), × = bulk sample (5 cm interval), × = monolith sample (0.75 cm interval). (b) Bioturbation features, + = very few, ++ = few, +++ = common, ++++ = frequent, +++++ = dominant, ++++++ = very dominant; and (c) calibrated radiocarbon ages (cal AD/BC) for the mineral soil profiles.

Table 2 Conventional (BP) and calibrated (cal AD/BC) radiocarbon ages of the humic acid fraction (except for samples located just beneath a thick ectorganic horizon where the humin fraction was dated, as indicated in bold font)

Site	Code[a]	Horizon[b]	Depth[c] (cm)	^{14}C age (BP)	δ^{13}C (‰)	Calibrated radiocarbon age		Reference[c]
						Range (cal AD/BC)	Mean (cal AD/BC)	
G1	**GrA-30094[e]**	**H**	**−30.5**	**40 ± 35**	**−25.73**	**cal AD 1877 to 1912**	**cal AD 1895**	
	GrA-30092	H	−1	380 ± 35	−25.68	cal AD 1449 to 1517	cal AD1483	
	GrA-34933	**Ah**	**0**	**1225 ± 40[f]**	**−28.15**	**cal AD 769 to 830**	**cal AD 800**	
	GrA-34934	Ah	10	2475 ± 40	−27.18	cal BC 727 to 606	cal BC 667	
	GrA-34935	2Ahb	39	6155 ± 45	−25.31	cal BC 5135 to 5049	cal BC 5092	
G5a	GrA-30109	F	−20.5	−623 ± 35	−27.46	cal AD 1996 to 2002	cal AD 1999	*
	GrA-30112	F	−1	−28 ± 35	−26.39	cal AD 1956 to 1957	cal AD 1957	*
	GrA-34938	**Ah**	**5**	**325 ± 35[g]**	**−26.91**	**cal AD 1538 to 1602**	**cal AD 1570**	
	GrA-28101	**Ah**	**10**	**775 ± 35[h]**	**−25.93**	**cal AD 1247 to 1271**	**cal AD 1259**	*
	GrA-34939	Ah	20	755 ± 35	−26.51	cal AD 1251 to 1281	cal AD 1266	
	GrA-30113	Ah	24.5	355 ± 35	−26.03	cal AD 1467 to 1523	cal AD 1495	**
	GrA-30114	Ah	39.5	1855 ± 40	−26.65	cal AD 124 to 217	cal AD 171	**
	GrA-28104	Bw	49.5	2170 ± 35	−25.92	cal BC 352 to 293	cal BC 323	*
	GrA-30133	1/2 Bw	69	3650 ± 40	−25.71	cal BC 2041 to 1956	cal BC 1999	**
	GrA-30134	1/2 Ah1b	70.5	3880 ± 40	−25.62	cal BC 2406 to 2337	cal BC 2372	**
	GrA-28108	1/2 Ah1b	79.5	4355 ± 40	−25.10	cal BC 3015 to 2944	cal BC 2980	*
	GrA-34943	2Ah1b	85	4870 ± 40	−25.57	cal BC 3667 to 3638	cal BC 3653	
G5b	GrA-35329	Ah	5	200 ± 35	−25.86	cal AD 1766 to 1801	cal AD 1784	
	GrA-35330	Ah	10	400 ± 35	−25.88	cal AD 1441 to 1494	cal AD 1468	
	GrA-30138	Ah	14.5	590 ± 35	−25.33	cal AD 1311 to 1359	cal AD 1335	*
	GrA-35354	Ah	20	685 ± 35	−25.62	cal AD 1276 to 1300	cal AD 1288	
	GrA-35355	Ah	25	855 ± 35	−25.75	cal AD 1157 to 1224	cal AD 1191	
	GrA-28111	Ah	34.5	1350 ± 35	−25.45	cal AD 648 to 682	cal AD 665	*
	GrA-30139	Bw1	49.5	2070 ± 40	−26.45	cal BC 116 to 43	cal BC 80	**
	GrA-30107	Bw1	64.5	3045 ± 40	−25.79	cal BC 1323 to 1266	cal BC 1295	**
	GrA-28113	1/2 Bw2	75	3465 ± 35	−25.51	cal BC 1780 to 1740	cal BC 1760	*
	GrA-30238	1/2 Bw2	94.5	4270 ± 40	−25.81	cal BC 2913 to 2879	cal BC 2896	**
	GrA-30232	1/2 Bw2	114	5260 ± 40	−24.81	cal BC 4071 to 4034	cal BC 4053	**
	GrA-30234	2Ahb	115.5	5405 ± 40	−25.20	cal BC 4327 to 4280	cal BC 4304	**
	GrA-28116	2Ahb	124.5	5730 ± 40	−24.91	cal BC 4614 to 4515	cal BC 4565	*
G7	GrA-28130	Ah1	10	180 ± 35	−25.24	cal AD 1761 to 1789	cal AD 1775	*
	GrA-28134	Ah2	46.5	1690 ± 40	−25.22	cal AD 329 to 407	cal AD 368	*
	GrA-28126	1/2 Ahb	89.5	4910 ± 45	−24.98	cal BC 3712 to 3643	cal BC 3678	*
	GrA-34944	2Ahb	98	5985 ± 45	−25.47	cal BC 4935 to 4860	cal BC 4898	

[a]Laboratory code of the Centre for Isotope Research, Groningen University, the Netherlands.
[b]Horizon nomenclature of ectorganic horizons according to Green *et al.* (1993).
[c]Depth of sample, vertical sample interval 0.5 cm, the mineral soil surface was set at 0 cm, samples taken from soil monolith.
[d]*Tonneijck *et al.* (2006), **Tonneijck *et al.* (2007).
[e]In this case the humin fraction was dated because HA was lost.
[f]^{14}C age of HA was 840 ± 35 BP.
[g]^{14}C age of HA was 255 ± 35.
[h]^{14}C age of HA was 490 ± 35 BP.

ages of HA for the age-depth relationship in all cases, except for the mineral soils just beneath the ectorganic horizon of the forest profiles, where we used calibrated radiocarbon ages of humin instead, according to Tonneijck *et al.* (2006). The R^2 value of the linear regression was large in all cases (> 0.84). The slope of the age-depth relationship in the mineral soil of forest site G1 was significantly different from the slopes of the other soil profiles, while forest patch profile G5a resembled the páramo profiles.

Mineral and organic components

Throughout the mineral horizons of all soil profiles, mineral components (data not shown) were represented by plagioclase, amphibole, biotite, vesicular rhyolitic volcanic glass and rhyolitoid rock fragments. Opaque mineral grains (e.g. magnetite and hematite) were difficult to recognize because of the presence of very fine (< 20 μm) opaque OM fragments. In general, minerals and rock fragments showed only initial pellicular and/or dotted

weathering. Fine mineral components in the mineral horizons of all soil profiles consisted of dull light to dark brown, isotropic material with undifferentiated b-fabric. The presence of very fine (< 20 μm) opaque OM resulted in a dotted appearance.

Distribution of fresh roots and fragmented OM (as area %) as observed in the thin sections is presented in Figure 2. In the ectorganic horizons of the forest profiles, OM was mainly present as common fresh roots, frequent to common fragmented OM (both roots and leaves) and fine organic groundmass. In the mineral horizons of all soil profiles, the abundance of fresh roots and fragmented OM decreased quickly with depth from (very) few to common in the mineral topsoils to very few further down the soil profiles. Very few intact and fragmented sclerotia occurred throughout the mineral soil profiles. Additionally, very few irregular shaped opaque OM fragments of various sizes were present, mostly without recognizable cell structure.

Type and distribution of bioturbation features

The vertical distribution of bioturbation features (as area %), type of bioturbation features (as proportions of total) and microstructures (as area %) are presented in Figure 2 and described in detail for each soil profile in the following sections. Figure 3b shows bioturbation features versus depth.

G7 páramo. Within the first 3 cm of the Ah1 horizon, bioturbation features were frequent and occurred mainly as loose discontinuous infillings containing clustered spherical brown matric excrements (50–100 μm diameter) in varying stages of welding. Welding resulted in transformation to mammilated excrements, occurring again in clusters (Figure 4). In addition, very few organic/matric dark brown mammilated excrements up to ~8 mm diameter were present near the surface. This zone had a crumb microstructure and showed an irregular tonguing boundary along which massive dense complete matric infillings (~5 mm diameter) were observed, composed of fine brown groundmass with (very) few mineral grains and very few OM fragments. These dense infillings were similar in size and composition to the ones occurring at greater depth but had a mammilated outline owing to the greater porosity of the topsoil.

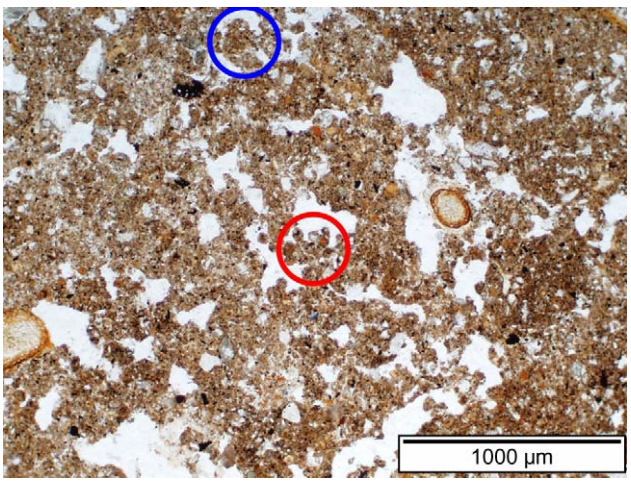

Figure 4 Current soil with páramo vegetation: loose discontinuous infillings with welded spherical (encircled in the middle of the graph) and mammilated excrements (encircled at top), eventually grading into a vughy microstructure.

Bioturbation features decreased with depth to few in the Ah horizon (at 30 cm depth), initially mainly occurring as loose discontinuous infillings with clustered spherical to mammilated excrements similar to the ones in the topsoil. These infillings were often welded to such an extent that a vughy microstructure developed (Figure 4). In addition, very few loose continuous infillings with welded matric spherical excrements (~100 μm diameter) occurred in clustered and banded basic distribution patterns. From 30 cm depth onwards, bioturbation features were mainly present as brown dense complete infillings instead of loose infillings.

Strikingly, dense complete infillings increased to dominant in the 1/2Ah2 and 1/2Ahb horizons (the overprinted zone), while loose discontinuous infillings were absent. The colour contrast between different dense infillings increased and they were now composed of either dark brown fine groundmass or brown to light brown fine groundmass (Figure 5a,b). The mineral grains sometimes showed a crescent distribution pattern following the outline of the dense infilling. In the overprinted zone a channel microstructure (Figure 6) became dominant. The randomly distributed channels ranged from 60 to 600 μm diameter and did not contain excrements; some channels did contain roots.

G5b páramo next to forest patch. The type and distribution of bioturbation features in profile G5b was very similar to profile G7 (see Figure 2). Within the first 2 cm of the Ah horizon, bioturbation features were frequent and the microstructure was crumb with few massive zones. Similar to G7, bioturbation features decreased with depth to very few at the bottom of the Ah horizon. Loose discontinuous infillings remained present until 35 cm. Microstructure changed to massive, with very few vughy zones where loose infillings became so strongly welded that they were no longer recognizable as such. The proportion of dense infillings was somewhat higher than that of loose infillings throughout the Ah horizon. As in profile G7, from the Bw horizon onwards bioturbation features increased and occurred only as light brown to dark brown dense infillings. However, the frequency of bioturbation features in the overprinted zone was somewhat lower than in G7. Colour contrast between the dense infillings increased with depth throughout the profile. At depth, a similar channel microstructure as in profile G7 became dominant.

G1 forest. Within the first 5 cm of the thick (75 cm) ectorganic profile of G1, bioturbation features were frequent and represented by both single and welded excrements. Microstructure

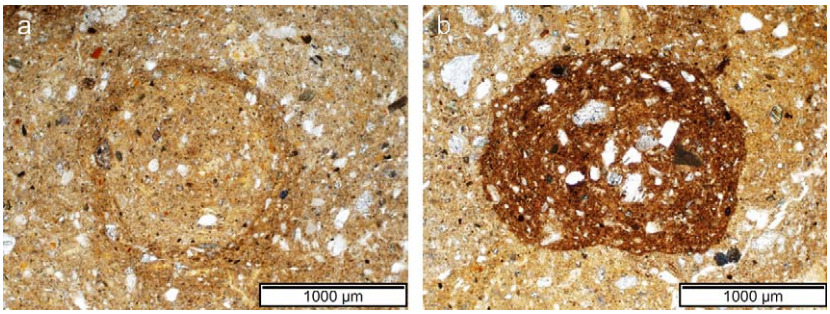

Figure 5 Current soils with páramo vegetation and overprinted zones of all soil profiles: (a) brown dense complete infilling and (b) dark brown dense complete infilling with coarser texture; dense infillings resulted in a massive microstructure.

was crumb. We encountered small spherical/ellipsoidal organic excrements, ranging from 50–200 µm diameter. Such excrements were composed of light brown to reddish brown organic fine groundmass without recognizable OM fragments, often associated with leaf and root tissues (Figure 7). In addition, larger mammilated organic excrements (up to 800 µm diameter) composed of light brown to reddish brown organic fine groundmass with common OM fragments occurred. Welding increased quickly with depth.

Further down the ectorganic horizons, the mammilated organic excrements became so strongly welded that they turned into fine organic groundmass mostly without recognizable excrements. The microstructure became massive in large parts of the thin sections. These massive zones did not qualify as 'bioturbation feature' according to our definition, because (welded) excrements were no longer recognizable as such. Bioturbation features decreased with depth to very few. Still, very few single to strongly welded organic spherical/ellipsoidal excrements were present even at the bottom of the ectorganic horizons, often associated with roots and leaf fragments.

In the Ah horizon, very few bioturbation features were present as loose discontinuous infillings composed of (very strongly) welded bright reddish brown spherical organic/matric excrements, and microstructure was massive. The fine groundmass was of similar colour to these excrements and the boundaries between infillings and fine groundmass were diffuse. The transition between ectorganic and mineral horizons was gradual, the Ah horizon still containing common fresh roots and fragmented OM.

In the 1/2Bw horizon (overprinted zone), bioturbation changed drastically with regard to type of activity, and increased in abundance to very dominant. Bioturbation features were only present as dense complete matric infillings of the same types as encountered in profiles G7 and G5b. Bioturbation features in the 2Ahb horizon were very similar to those in the overlying 1/2Bw horizon.

G5a forest patch. In the ectorganic horizons of profile G5a, similar types of bioturbation features were present as in forest profile G1. We observed that the mammilated organic excrements were often composed of smaller excrements, which was not clear in profile G1, probably through stronger welding there. In contrast to G1, we did not observe zones with massive microstructure and excrements remained recognizable. Bioturbation features remained frequent to dominant throughout the ectorganic horizons.

The mineral topsoil of forest patch G5a resembled páramo profiles G7 and G5b rather than forest profile G1. At the top of the Ah horizon, bioturbation features were frequent, occurring as loose discontinuous infillings similar to the ones found in páramo profiles G7 and G5b. They were again often welded to such an extent that a vughy microstructure developed. In contrast to profile G1, the transition between ectorganic and mineral horizons was abrupt, the Ah horizon containing only very few fresh roots and fragmented OM and lacking the reddish staining. With depth, the loose infillings decreased in abundance until they disappeared in the 1/2 Bw horizon. Instead, very few dense complete matric infillings similar to the ones encountered in profile G7 appeared at the bottom of the Ah horizon. These dense infillings became dominant in the Bw horizon and very dominant in the 1/2Bw and 1/2Ah1b horizons (overprinted zone). Simultaneously, microstructure changed to massive with depth. Finally, in the 2Ah2b horizon dense infillings decreased somewhat in abundance to frequent and a channel microstructure developed. The colour contrast between dense infillings increased with depth.

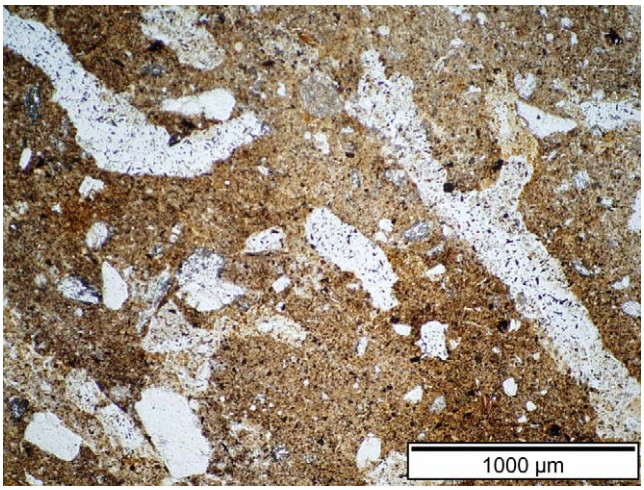

Figure 6 Overprinted zones and top of palaeosol: channel microstructure. NB: dotted appearance due to abrasive powder.

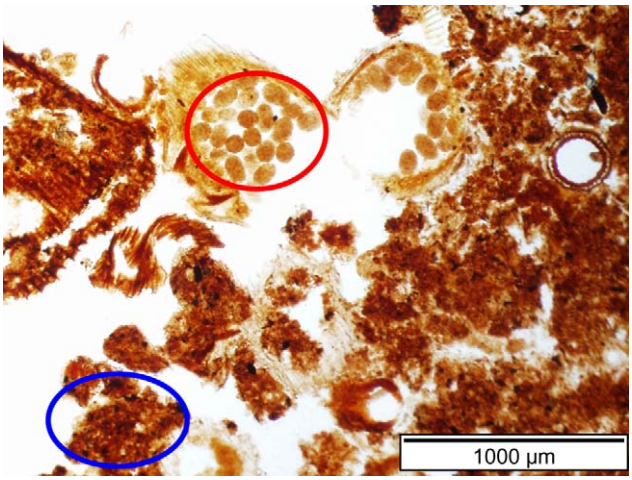

Figure 7 Ectorganic profile forest: ellipsoidal organic excrements (encircled at the top of the graph) and mammilated organic excrements (encircled left bottom corner).

Discussion

Mineral and organic components

Micromorphological observations of the mineral components confirmed the mineralogical assemblage as determined by X-ray diffraction and presented by Tonneijck *et al.* (2008). The dull light to dark brown colour of the fine groundmass indicated staining by OM, because organic carbon contents were high (> 6%) in all mineral horizons. A large organic carbon content is typical for Andosols and can be related to the formation of amorphous organo-mineral/metal complexes (Dahlgren *et al.*, 2004). Our conclusion with respect to staining by OM was confirmed by the undifferentiated b-fabric of the fine mineral components that indicated masking by humus and/or the presence of amorphous materials (Stoops, 2003). The red colouring of the fine groundmass in the mineral topsoil of forest site G1 was most likely from OM staining and not from the presence of iron, because amorphous Fe contents were low there and similar to the other topsoils lacking this red colouring (Tonneijck *et al.*, 2008). The irregular shaped opaque OM fragments may well be charcoal fragments, because páramo vegetation in the study area is known to be subject to burning and charcoal fragments were found by Di Pasquale *et al.* (2007) in soils from the same study area.

Soil faunal groups

Based on the distribution and composition of bioturbation features, we deduced which soil faunal group probably created them. This is of great importance, because it may clarify the vertical distribution of SOM (Anderson, 1988), as explained in the Introduction. Both in the mineral soil profiles and in the ectorganic horizons of the forest sites, the heterogeneity of the bioturbation features encountered indicated the activity of several soil faunal species. The small organic excrements occurring in the ectorganic horizons of the forest profile obviously were formed by epigeic species. The matric composition and random distribution of the small (50–100 µm diameter) excrements occurring as loose infillings in the Ah horizons clearly suggest that these were produced by small endogeic species. Similarly, the larger (~5 mm diameter) matric dense infillings were created by larger endogeic species, as indicated by their composition and dominant occurrence in the subsoil. As we did not observe permanent vertical burrows either in the thin sections or in the field, anecic species must have been scarce or absent. The dominant soil fauna is most likely represented by *Lumbricidae*, *Acari*, *Collembola*, *Enchytraeidae* and *Nematoda*, similar to Colombian (van der Hammen & Beglinger, 1989) and Mexican Andosols (Barois *et al.*, 1998). Detailed classification of soil faunal species is not possible because of the morphological similarity of soil faunal pedofeatures (Pawluk, 1987).

Vertical distribution of roots

The dominant occurrence of both fresh roots and fragmented OM (including roots and leaves) in the ectorganic horizons and/or mineral topsoil confirmed our field descriptions of superficial root distribution (Tonneijck *et al.*, 2006) and are in accordance with data from Soethe *et al.* (2006) for Ecuadorian montane forest and data from Hofstede & Rossenaar (1995) for Colombian páramo ecosystems. Páramo ecosystems have the highest above-ground:below-ground biomass ratio (typically 1:0.35) of a wide range of grassland ecosystems (Hofstede & Rossenaar, 1995).

As the channel microstructure that was present in the overprinted zone and top of the palaeosol (except in profile G1) was not accompanied by an increase in fresh roots (Figure 2) and channels were often empty, we conclude that the root system there is no longer in use. Because the channel microstructure occurred in both part of the current soil and the palaeosol, it was probably formed after the last tephra deposition. Possibly, roots have shifted upwards over time. Alternatively, a deeper rooting vegetation type in the past could have created the channel microstructure, although this seems unlikely in light of the superficial root systems of both current forest and páramo vegetation.

Nierop *et al.* (2007) found with analytical pyrolysis techniques that the subsoils of our soil profiles exhibited more of a root- than of a leaf-derived SOM type. Root litter may have been transported by bioturbation to the subsoil instead of being deposited there *in situ* and/or prior to upward shifting roots that may have reached the subsoil.

Vertical distribution of HA

The strong correlation between carbon in the HA fraction and total organic carbon in the mineral soil profiles demonstrates that HA was transported through the soil profile by the same

mechanisms as bulk SOM. Radiocarbon dating of HA therefore offers an additional clue regarding the vertical transport of bulk SOM. Radiocarbon dating of HA matched very well with dating of charcoal fragments in mineral soil profiles from the same research area by Di Pasquale *et al.* (2007), confirming the reliability of our datings. In a previous study (Tonneijck *et al.*, 2006) we already indicated that HA in these soils was most likely not rejuvenated by roots or illuviation of younger OM. Only the mineral topsoils just beneath the thick ectorganic horizons of the forest profiles formed an exception, as the younger age of HA than of the humin fraction there did indicate some illuviation of younger HA from the ectorganic horizons. Because of this, in those specific cases humin was used for dating.

Vertical distribution of SOM: ectorganic horizons

OM accumulation on top of the mineral soil surface demonstrated that bioturbation did not transport OM vertically in the forest sites (G1 and G5a). Indeed, the soil faunal pedofeatures in the ectorganic horizons were produced by epigeic species and these do not redistribute OM (Anderson, 1988). In the ectorganic horizons of forest profile G1, the strong increase in welding with depth to the extent that a massive microstructure developed, suggested that bioturbation is no longer active at depth. However, the frequent occurrence of fragmented OM tissue and the decrease in size of fragmented OM showed that bioturbation must once have been more active. Apparently, bioturbation mainly affects fresh OM continuously supplied at the surface, rather than older OM (up to 1483 cal AD, Table 2) remaining at depth. Additionally, the very acidic pH (pH $CaCl_2 < 2.5$) and periodically wet and anaerobic conditions in the thick ectorganic horizons are unfavourable for soil faunal activity. At forest patch G5a, the ectorganic horizon was thinner (35 cm) than at G1 and much younger, its base dated to 1957 cal AD (Table 2). Because OM was still relatively fresh, bioturbation features were more frequent than at G1. The site also had a better drainage, resulting in less welding of excrements as compared with profile G1. Bioturbation throughout the ectorganic horizons of G5a is probably still active, although it does not result in vertical transport of OM.

Vertical distribution of SOM: current soils

Pessenda *et al.* (2001) and Rumpel *et al.* (2002) found a similar increase in age with depth accompanied by a decrease in organic carbon content, as in our current mineral soil profiles, and related this to a larger input of younger material to the topsoil than to the subsoil. In our case this could have been caused by the decrease in bioturbation (loose infillings) with depth combined with dominant OM input from the soil surface (above-ground litter) and topsoil (superficial rooting). Additionally, at the forest sites (G1 and G5a) some OM illuviation in the mineral topsoil occurred, as explained previously.

The rejuvenating impact of fresh OM increases with increasing age difference (Mook & Van de Plassche, 1986). Apparently, bioturbation seldom transports fresh OM directly to the older subsoil, even though some bioturbation features were found there. Indeed, fresh OM was concentrated in the topsoil and loose and dense infillings in the current soils were mainly composed of matric rather than organic material. The endogeic species observed to be dominant in the studied soil profiles feed on SOM rather than fresh OM from the earth surface (Anderson, 1988; Lavelle, 1988, Lee & Foster, 1991). Mixing of SOM with small age differences over short distances does not prevent a linear age-depth relationship even if bioturbation extends to considerable depth. Thus, downward SOM transport must have occurred largely in the chronological order in which it was supplied at the surface, gradually moving deeper into the soil.

Vertical distribution of SOM: overprinted zones

In the overprinted zone, the unusual increase of organic carbon with depth suggested that soil fauna mixed the subsoil of the current soil with the topsoil of the palaeosol (Tonneijck *et al.*, 2008), which was confirmed by our micromorphological observations. Material with a relatively low organic carbon content and relatively young age (bottom of the current soil) was mixed into material with a higher organic carbon content and relatively high age (palaeosol), as suggested by the occurrence of dense infillings of contrasting colour. Current roots were mainly concentrated in the topsoil (páramo) and ectorganic horizons (forest), but past roots may have contributed to the increase in organic carbon in the overprinted zone, as suggested by the channel microstructure. However, root input alone cannot readily explain the gradual nature of this increase and therefore bioturbation is probably of overriding importance.

We discarded two remaining possibilities that in theory could have caused the unusual distribution of organic carbon contents in the overprinted zone (Tonneijck *et al.*, 2008). First, while burial of a páramo vegetation would probably not result in elevated organic carbon contents, one can imagine that burial of a thick ectorganic horizon could. However, in that case the lithology should be that of the tephra deposit burying it, which was not supported by grain size and geochemical data. Moreover, buried ectorganic horizons would be recognizable as such with micromorphological analysis. Second, as mentioned before, leaching and subsequent illuviation of OM is highly unlikely in Andosols because of the large metal-to-SOM ratios (Aran *et al.*, 2001; Dahlgren *et al.*, 2004) and indeed we did not observe any signs of OM illuviation (e.g. coatings) in our micromorphological analysis. Rumpel *et al.* (2002) presented data on a Podzol profile with leaching as the dominant mode of OM transport and illuviation of younger OM resulted in a radiocarbon age inversion. Such age inversions were not observed in the overprinted zone.

In view of the magnitude of bioturbation in the overprinted zone, one would expect the entire overprinted zone to have been

homogenized, which clearly contradicts the observed gradual increase in organic carbon. In addition, if bioturbation indeed had resulted in complete homogenization of the overprinted zone, one would not expect to find a linear age-depth relationship but rather one average age. At the very least one would have expected to find some age inversions, which was not the case. Apparently, analogous to overlying horizons, mixing in the overprinted zone occurred only over short vertical distances. The observed increase in contrast between dense infillings with depth indeed fits short vertical distance mixing, because the colour contrast between the bottom of the current soil and top of the palaeosol must have been greater than the contrast between different positions within the current soil itself. Indeed, the endogeic species dominant in the profiles studied mainly move horizontally and are not responsible for transport over large vertical distances (Anderson, 1988).

In the top of the palaeosol, a channel microstructure was superimposed on the dense infillings. Because the channel microstructure was related to the former presence of roots, as explained previously, this implies that the dense infillings were not recently made. The simultaneous occurrence of channel microstructures and massive microstructures in the overprinted zone between the current soil and palaeosol, suggest that either the root system was less extensive or that part of the dense infillings were formed relatively recently. The latter explanation seems more likely because roots generally decrease rather than increase with depth. Possibly the zone with the dense infilling type of bioturbation has shifted upwards over time.

Short vertical distance mixing

Both in the current soils (mineral horizons) and the overprinted zones, our results suggest that mixing by endogeic species occurred only over short vertical distances. Even though bioturbation differed greatly in magnitude throughout the soil profiles, being much more extensive in the overprinted zone, the slope of the linear age-depth relationship was not much affected. This implies that the vertical interval of mixing (i.e. the age differences mixed) was small and similar throughout the soil profile. As both radiocarbon ages and organic carbon contents were not homogenized over vertical intervals of 5 cm, we conclude that mixing must have occurred over even smaller distances.

An additional process explaining mixing over short vertical distances could be an upward shift of the soil fauna, rendering deeper positions in the soil out of reach of bioturbation over time. The channel microstructure superimposed on the dense infillings and vice versa indeed suggested upward shifting. Upward shifting may have been caused by soil thickening due to SOM accumulation (Tonneijck *et al*., 2008). Such soil thickening has been observed in Mexican volcanic ash soils as well (Barois *et al*., 1998). Another explanation for upward shifting could be that soil fauna itself migrated upwards in response to changes in hydrology over time (e.g. such as caused by the formation of an impermeable placic horizon as encountered in the soils studied).

Spatial variability of bioturbation features

Micromorphological studies are typically not suited to account fully for the spatial variability of pedofeatures, because of the small number of samples and replicates involved. However, we do not expect great variability of bioturbation features within the soil horizons, because we observed in the field that the variability of soil properties within horizons (e.g. very fine to medium root distribution, soil moisture, porosity, structure, and colour) was small. Our micromorphological results indeed showed that the variability of bioturbation features in the overprinted zone was small, because bioturbation features occupied a high proportion of the thin sections in all soil profiles studied (see Figure 2). The spatial variability of bioturbation features in the current soils may be somewhat greater because of their lower abundance. However, the cumulative effect of localized bioturbation features over time decreases the spatial variability if they are randomly distributed, which is likely because they were formed by endogeic species. Still, the possibility exists that we missed bioturbation features that were less abundant, but these scarce features would then probably not exert a strong influence on the vertical distribution of SOM. Overall, the general trends in the vertical distribution of SOM (i.e. decreasing in the current soil profiles and increasing in the overprinted zones) can largely be explained by our micromorphological observations of bioturbation features.

Vegetation type and soil fauna

Vegetation type indirectly influences the soil fauna because of the palatability of its litter (Swift *et al*., 1979). The sites studied were located along an altitudinal transect intersecting the upper forest line. Altitudinal fluctuations of this upper forest line result in a complex vegetation history at our sites (Di Pasquale *et al*., 2007; Bakker *et al*., 2008; Jansen *et al*., 2008), which is reflected by changes in soil faunal pedofeatures.

At the páramo sites above the current upper forest line (G5b and G7) both loose infillings and dense infillings produced by endogeic species were present up to the soil surface, while they were absent at the surface of the forest sites. This suggests that endogeic species are still active today in the páramo ecosystem while they are not active anymore in the forest. Instead, epigeic species dominate the forest soils, eventually resulting in the formation of thick ectorganic horizons because epigeic species do not redistribute OM (Anderson, 1988). Site G5a was only relatively recently colonized by forest vegetation (Jansen *et al*., 2008), which probably explains why the mineral soil profile of G5a resembled the mineral soil profiles of páramo (G5b and G7) rather than forest (G1) with regard to the soil faunal pedofeatures encountered and the slope of the age-depth relationship.

The deviating slope of the age-depth relationship in the mineral soil of forest site G1 was probably related to dominant accumulation of OM on the surface of the soil instead of within

the mineral soil for a prolonged period of time. Indeed, the age-depth relationship in the forest profile of Di Pasquale *et al.* (2007), with an equally thick ectorganic layer, had a similar deviating slope. Still, the sudden appearance of dense infillings at depth in forest profile G1 could indicate the former presence of páramo vegetation even at this low altitude site. In view of the thickness of the ectorganic profile and the gradual transition from ectorganic to mineral horizons in G1, such páramo vegetation would predate that of site G5a. Di Pasquale *et al.* (2007) indeed suggested that páramo was present before ~3900 cal BC at their currently forested site at similar low altitude (3540 m above sea level) in the same study area. Similarly, pollen analysis of a small mire in our study area indicated that the upper forest line was located at a low altitude (between 3100 and 3300 m above sea level) both before ~4300 cal BC and between ~210 cal BC and ~1430 cal AD (Bakker *et al.*, 2008). Thus, site G1 could well have been covered by páramo vegetation during these periods.

Implications

Vertical transport of SOM by bioturbation is often modelled with diffusion equations that use uniform diffusion coefficients with depth (e.g. Elzein & Balesdent, 1995; Bruun *et al.*, 2007). However, in our case this would have resulted in a vertical distribution of SOM with smooth turning points rather than in the observed sharp turning points. Modelling of the vertical distribution of SOM in our soils, and probably in volcanic ash soils in general, may be greatly enhanced by applying diffusion coefficients changing with depth as based on observed bioturbation features, in combination with soil thickening and subsequent upward shifting of bioturbation.

The studied soil profiles contain palaeoecological proxies (e.g. pollen and biomarkers) that are used to reconstruct the vegetation history in the study area (Jansen *et al.*, 2008). As the use of palaeoecological proxies contained in soils depends *inter alia*. on their preservation in chronostratigraphic order, the degree and type of bioturbation is of key importance. The results from the present study suggest that as long as palaeoecological proxies are transported through the soil profile in a similar way to bulk SOM and HA, they will be distributed in a (crude) chronostratigraphic order. However, a major consequence of the present research with respect to palaeoecological investigations is also that any sample taken inevitably would produce a mixed signal.

Conclusions

The páramo soil data suggest that bioturbation was largely responsible for the vertical distribution of SOM, while illuviation and root input were of minor importance. In the mineral topsoils, a decrease in bioturbation by small endogeic species with depth combined with dominant OM supply from the soil surface and topsoil resulted in a decrease in organic carbon content and an increase of age with depth. In the overprinted zone, our data suggest that extensive bioturbation by larger endogeic species mixed the initially relatively SOM-poor subsoil with the SOM-rich underlying palaeosol, which resulted in a gradual increase in organic carbon content with depth. Our data additionally suggest that mixing throughout the soil profile occurred only over short (< 5 cm) vertical distances. Short vertical distance mixing was apparently enhanced by upward shifting of bioturbation as a result of soil thickening due to SOM accumulation. A change from páramo to forest vegetation was accompanied by a change from endogeic to epigeic species. These latter species do not redistribute material vertically, which eventually resulted in the formation of thick ectorganic horizons in the forest.

Acknowledgements

We acknowledge the Ecuadorian Ministerio del Ambiente for issuing the necessary permits, Jatun Sacha for their support in Guandera Biological Station and Ecopar for their office assistance. Furthermore, we acknowledge the fellow members of the RUFLE programme, Jan Sevink, Koos Verstraten, Boris Jansen, Marcela Moscol Olivera, Henry Hooghiemstra and Antoine Cleef, for their valuable contributions to this research. In this respect we also thank Emiel van Loon, Misha Velthuis, Mirjam Pulleman, Jan Peter Lesschen and Kasper de Rooy. Finally, we wish to thank Leo Hoitinga for his assistance in the chemical laboratory and Frans Backer and Wijnanda Koot for thin section preparation. This research was funded by WOTRO (WAN 75-405) and the University of Amsterdam and generously sponsored by Fjällraven in the form of clothing and gear.

References

Anderson, J.M. 1988. Invertebrate-mediated transport processes in soils. *Agriculture, Ecosystems & Environment*, **24,** 5–19.

Aran, D., Gury, M. & Jeanroy, E. 2001. Organo-metallic complexes in an Andosol: a comparative study with a Cambisol and Podzol. *Geoderma*, **99,** 65–79.

Bakker, J., Moscol Olivera, M. & Hooghiemstra, H. 2008. Holocene environmental change at the upper forest line in northern Ecuador. *The Holocene* (in press).

Barois, I., Dubroeucq, D., Rojas, P. & Lavelle, P. 1998. Andosol-forming process linked with soil fauna under the perennial grass *Mulhembergia macroura*. *Geoderma*, **86,** 241–260.

Bruun, S., Christensen, B.T., Thomsen, I.K., Jensen, E.S. & Jensen, L.S. 2007. Modeling vertical movement of organic matter in a soil incubated for 41 years with ^{14}C labeled straw. *Soil Biology & Biochemistry*, **39,** 368–371.

Dahlgren, R., Saigusa, M. & Ugolini, F. 2004. The nature, properties and management of volcanic soils. *Advances in Agronomy*, **82,** 113–182.

Di Pasquale, G., Marziano, M., Impagliazzo, S., Lubritto, C., de Natale, A. & Bader, M.Y. 2007. The Holocene treeline in the Northern Andes (Ecuador): First evidence from soil charcoal. *Palaeogeography, Palaeoclimatology, Palaeoecology*, **259,** 17–34.

Elzein, A. & Balesdent, J. 1995. Mechanistic simulation of vertical distribution of carbon concentrations and residence times in soils. *Soil Science Society of America Journal*, **59,** 1328–1335.

FAO 2006. *World Reference Base for Soil Resources 2006. A Framework for International Classification, Correlation and Communication*. World Soil Resources Reports No 103, FAO/ISRIC/IUSS, Rome.

Green, R.N., Trowbridge, R.L. & Klinka, K. 1993. Towards a taxonomic classification of humus forms. In: *Forest Science Monograph 29* (eds W.F. Hyde, K.W. Winget & B. Smith), pp. 1–50. Society of American Foresters, Washington, DC.

Hofstede, R.G.M. & Rossenaar, A.J.G.A. 1995. Biomass of grazed, burned and undistubed paramo grasslands, Colombia. II. Root mass and aboveground:belowground ratio. *Arctic & Alpine Research*, **27,** 13–18.

Jansen, B., Haussmann, N.S., Tonneijck, F.H., Verstraten, J.M. & De Voogt P. 2008. Characteristic straight-chain lipid ratios as a quick method to assess past forest – páramo transitions in the Ecuadorian Andes. *Palaeogeography, Palaeoclimatology, Palaeoecology*, **262,** 129–139.

Keese, J., Mastin, T. & Yun, D. 2007. Identifying and assessing tropical Montane forests on the Eastern Flank of the Ecuadorian Andes. *Journal of Latin American Geography*, **6,** 63–83.

Lavelle, P. 1988. Earthworm activities and the soil system. *Biology & Fertility of Soils*, **6,** 237–251.

Lee, K.E. 1959. The earthworm fauna of New Zealand. *Bulletin of the New Zealand Department of Scientific and Industrial Research*, **130**.

Lee, K.E. & Foster, R.C. 1991. Soil fauna and soil structure. *Australian Journal of Soil Research*, **29,** 745–775.

Miedema, R., Pape, T. & Van de Waal, G.J. 1974. A method to impregnate wet soil samples, producing high-quality thin sections. *Netherlands Journal of Agricultural Science*, **22,** 37–39.

Mook, W.G. & Van de Plassche, O. 1986. Radiocarbon dating. In: *Sea-Level Research: A Manual for the Collection and Evaluation of Data* (ed. O. Van de Plassche), pp. 525–560. Geo Books, Norwich.

Murphy, C.P. 1986. *Thin Section Preparation of Soils and Sediments*. AB Academic Publishers, Berkhamsted.

Myers, N., Mittermeier, R.A., Mittermeier, C.G., da Fonseca, G.A.B. & Kent, J. 2000. Biodiversity hotspots for conservation priorities. *Nature*, **403,** 853–858.

Nierop, K.G.J., Tonneijck, F.H., Jansen, B. & Verstraten, J.M. 2007. Organic matter in volcanic ash soils under forest and paramo along an Ecuadorian altitudinal transect. *Soil Science Society of America Journal*, **71,** 1119–1127.

Pawluk, S. 1987. Faunal micromorphological features in moder humus of some Western Canadian soils. *Geoderma*, **40,** 3–16.

Pessenda, L.C.R., Gouveia, S.E.M. & Aravena, R. 2001. Radiocarbon dating of total soil organic matter and its comparison with ^{14}C ages of fossil charcoal. *Radiocarbon*, **43,** 595–601.

Rasse, D.P., Mulder, J., Moni, C. & Chenu, C. 2006. Carbon turnover kinetics with depth in a French loamy soil. *Soil Science Society of America Journal*, **70,** 2097–2105.

Rumpel, C., Kogel-Knabner, I. & Bruhn, F. 2002. Vertical distribution, age, and chemical composition of organic carbon in two forest soils of different pedogenesis. *Organic Geochemistry*, **33,** 1131–1142.

Schnitzer, M. 1982. Organic matter characterization. In: *Methods of Soil Analysis. Part 2: Chemical and Microbiological Properties* (ed. A. Page), pp. 581–594. American Society of Agronomy, Soil Science Society of America, Madison, WI.

Soethe, N., Lehmann, J. & Engels, C. 2006. The vertical pattern of rooting and nutrient uptake at different altitudes of a south Ecuadorian Montane forest. *Plant & Soil*, **286,** 287–299.

Stoops, G. 2003. *Guidelines for Analysis and Description of Soil and Regolith Thin Sections*. Soil Science Society of America Inc., Madison, WI.

Swift, M.J., Heal, O.W. & Anderson, J.M. 1979. *Decomposition in Terrestrial Ecosystems. Studies in Ecology*. Blackwell Scientific Publications, Oxford.

Tonneijck, F.H., Van der Plicht, J., Jansen, B., Verstraten, J.M. & Hooghiemstra, H. 2006. Radiocarbon dating of soil organic matter fractions in Andosols in Northern Ecuador. *Radiocarbon*, **48,** 337–353.

Tonneijck, F.H., Hageman, J.A., Sevink, J. & Verstraten, J.M. (2008) Tephra stratification of volcanic soils in Northern Ecuador. *Geoderma*, **144,** 231–247.

Van der Hammen, T. & Beglinger, E. 1989. Soil fauna in the Parque los Nevados transect. In: *Studies on Tropical Andean Ecosystems* (eds T. Van der Hammen, S Diaz-Piedrahita & V. Julio Alvarez), pp. 443–454. Gebrüder Borntraeger, Berlin.

Wang, Y.R., Amundson, R. & Trumbore, S. 1996. Radiocarbon dating of soil organic matter. *Quaternary Research*, **45,** 282–288.